

# Quadrupole Shift of Nuclear Magnetic Resonance of Donors in Silicon at Low Magnetic Field

P. A. Mortemousque,<sup>1</sup> S. Rosenius,<sup>1</sup> G. Pica,<sup>2</sup> D. P. Franke,<sup>3</sup> T. Sekiguchi,<sup>1,\*</sup> A. Truong,<sup>1</sup> M. P. Vlasenko,<sup>4</sup> L. S. Vlasenko,<sup>4</sup> M. S. Brandt,<sup>3</sup> R. G. Elliman,<sup>5</sup> and K. M. Itoh<sup>1</sup>

<sup>1</sup>*School of Fundamental Science and Technology, Keio University,  
3-14-1 Hiyoshi, Kohoku-ku, Yokohama 223-8522, Japan*

<sup>2</sup>*SUPA, School of Physics and Astronomy, University of St Andrews, KY16 9SS, United Kingdom*

<sup>3</sup>*Walter Schottky Institut, Technische Universität München, Am Coulombwall 4, 85748 Garching, Germany*

<sup>4</sup>*A. F. Ioffe Physico-Technical Institute, Russian Academy of Sciences, 194021, St. Petersburg, Russia*

<sup>5</sup>*Australian National University, Research School of Physics and Engineering, Canberra, ACT 0200, Australia*

Above megahertz shifts of nuclear magnetic resonance lines of antimony and bismuth donors in silicon are reported. Defects created by ion implantation of the donors are discussed as the source of effective electric field gradients generating these shifts. The experimental results are modeled quantitatively by molecular orbital theory for a coupled pair consisting of a donor and a spin-dependent recombination readout center.

Group-V donors are the most studied impurities in silicon (Si). For decades, the shallow donors have been employed for the fabrication of transistors in microelectronics. More recently, shallow donors have become very promising candidates as quantum bits (qubits) [1], since they can be considered as hydrogen-like atoms embedded in a solid-state matrix. The weak spin-orbit coupling present in the silicon host makes the coherence time of the donor electron and nuclear spins exceptionally long [2, 3]. Moreover, the existence of spin-free <sup>28</sup>Si allows for the isotopic purification of Si [4–6], further improving these coherence times by removing the residual nuclear spins of <sup>29</sup>Si (with a nuclear spin  $I = 1/2$ ) [7–11]. This has motivated researchers to investigate techniques to incorporate donors in silicon in order to produce single donor devices [12–14]. The electron and nuclear spin  $g$ -factors of shallow donors are already well-known [15]. Similarly, the hyperfine interaction between the donor electron with donor nuclear spin [15, 16] and with <sup>29</sup>Si nuclear spins [17] have been measured and are used to understand the donor electron wavefunction [18, 19]. More recently, the Stark shift of the donor states has been observed [20–22] and modeled [23–27].

This letter reports the experimental observation of line shifts of the nuclear spin resonance of <sup>121</sup>Sb, <sup>123</sup>Sb and <sup>209</sup>Bi donors in silicon at low magnetic fields observed via the electrical detection of mixed spin states. These shifts are interpreted as resulting from the nuclear electric quadrupole interaction (QI) of the nuclear quadrupole moment with the electron wavefunction, which is modified by the presence of implantation defects. A shift of the nuclear magnetic resonance (NMR) due to QI arises from the interaction of a nuclear spin  $I \geq 1$  with an electric field gradient (EFG) and is well-studied in the atomic physics and nuclear magnetic resonance commu-

nities [28–30]. However, the observation of a quadrupole-induced shift of the group-V donor NMR in silicon, where the QI with crystal field gradients vanishes due to the cubic symmetry, has only recently been realized for ionized donors in strained Si [31]. While an external application of EFG large enough to result in an observable shift ( $\gtrsim 10^{18}$  V/m<sup>2</sup>) is challenging, gradients of such a magnitude can be generated by donor electrons whose spatial symmetry is broken by the presence of strain [32], close acceptors [33] or defects created by ion implantation [34–36]. As our detection method is based on the spin-dependent recombination (SDR) [37–39] of close pairs formed by the donor electron and such defects, only donors that are exposed to these EFG are probed. By working at low magnetic fields, where the donor electron and nuclear spin wavefunctions mix strongly due to the hyperfine interaction, we are able to use such SDR signal to investigate possible quadrupole-induced NMR shifts [38].

Three samples, labeled Si:<sup>121</sup>Sb, Si:<sup>123</sup>Sb, and Si:<sup>209</sup>Bi, were employed in this study. The Si wafer used as a substrate to fabricate the samples was from highly resistive ( $> 3$  k $\Omega$ ·cm) float-zone Si. The samples were ion-implanted with <sup>121</sup>Sb, <sup>123</sup>Sb or <sup>209</sup>Bi at room temperature. Bi was implanted at 300 and 550 keV with doses of  $0.7 \times 10^{13}$  and  $1.3 \times 10^{13}$  cm<sup>-2</sup>, respectively. The isotope-selective Sb implantations were performed with an energy of 30 keV and a fluence of  $1.7 \times 10^{11}$  cm<sup>-2</sup>. These conditions yielded a maximum bismuth plateau-like concentration of  $1.8 \times 10^{18}$  cm<sup>-3</sup> (above the solubility limit [40]) in a depth of 90 to 150 nm from the surface, and a <sup>121,123</sup>Sb peak concentration of  $1.1 \times 10^{17}$  cm<sup>-3</sup> 24 nm from the surface. The three samples were individually annealed after the ion implantation, at 650 °C for 30 min in an evacuated quartz tube. This process, designed to maximize the number of donor-readout center (D–R) pairs [41], led to an activation efficiency [42–45] below 60%, resulting in a Bi donor concentration less than  $1.1 \times 10^{18}$  cm<sup>-3</sup>, and a <sup>121</sup>Sb and a Si:<sup>123</sup>Sb concentration less than  $4 \times 10^{16}$  cm<sup>-3</sup> (in all cases below

\* Present address: Institute for Integrated Cell-Material Sciences (WPI-iCeMS), Kyoto University, Yoshida-Honmachi, Sakyo-ku, Kyoto 606-8501, Japan

the metal-insulator transitions [46, 47]).

In the SDR detection technique, the photocarriers generated in the sample by a 100-W halogen lamp are captured by the ionized donors. The recombination time of the donor electrons depends on the relative electron spins of the donor and the paramagnetic readout center: in this donor-readout center pair, the antiparallel electron spin configuration leads to a fast recombination, whereas for the parallel spins the expected recombination time is much longer (spin blockade) [48]. For a continuous illumination, only the parallel electron spin pairs remain in the resulting steady state without external induction of magnetic resonance. Therefore, flipping the donor electron spins by magnetic resonance enhances the electron recombination, leading to a decrease in the sample photoconductivity from the steady state. This change in photoconductivity was measured by probing the change in the microwave reflectivity of the sample. The measurements were performed using a JEOL JES-RE3X X-band cw-electron spin resonance (ESR) spectrometer with an Oxford  $^4\text{He}$ -cryostat and a lock-in amplifier using a modulation amplitude of 7 G at 100 kHz. For the low frequency excitations, a coil placed on top of the sample was used. A static magnetic field is applied in the crys-

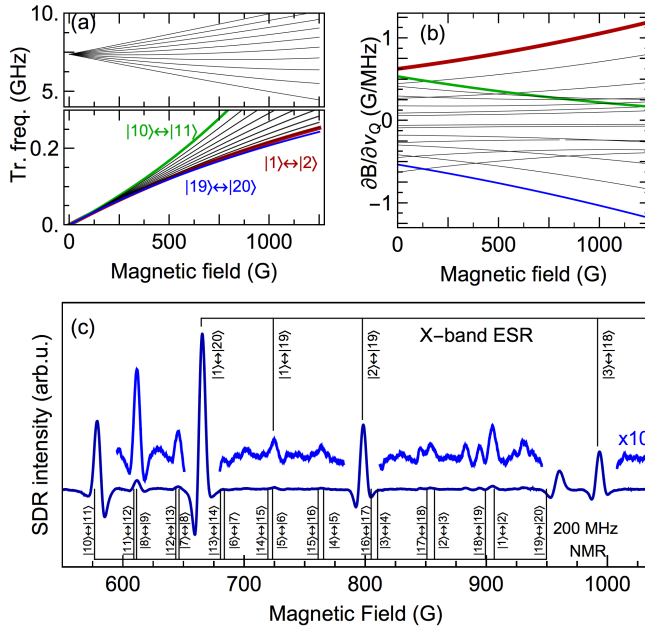


FIG. 1. (Color online.) (a) ESR (top) and NMR (bottom) transition frequencies and (b) NMR resonant magnetic field sensitivity to the QI of Bi donors as a function of magnetic field. The colored lines ( $|19\rangle \leftrightarrow |20\rangle$  in blue,  $|10\rangle \leftrightarrow |11\rangle$  in green and  $|1\rangle \leftrightarrow |2\rangle$  in red) have high SDR intensities and were analysed in this study. The same color code is used in Fig. 2(a, b and d). (c) Experimentally observed SDR spectrum of the Bi donor spin transitions under 200-MHz excitation. The black lines represent the expected resonance position of the electron and nuclear spin transitions without exchange interaction or QI.

TABLE I. Magnetic resonance parameters of  $^{75}\text{As}$ ,  $^{121}\text{Sb}$ ,  $^{123}\text{Sb}$  and  $^{209}\text{Bi}$  donor spins in silicon. The quadrupole moment of the donor nuclei  $Q$  is given in barn.  $\bar{a}_l$  are the Bohr radii (see Ref. 27).

	Si: $^{75}\text{As}$	Si: $^{121}\text{Sb}$	Si: $^{123}\text{Sb}$	Si: $^{209}\text{Bi}$
$I$	3/2	5/2	7/2	9/2
$g_e$	1.99837 <sup>a</sup>	1.9986 <sup>a</sup>	2.00049(5) <sup>b</sup>	
$g_n$	0.9596 <sup>a</sup>	1.3454 <sup>a</sup>	0.7285 <sup>a</sup>	0.9135 <sup>c</sup>
$A$ (MHz)	198.35 <sup>a</sup>	186.80 <sup>a</sup>	101.52 <sup>a</sup>	1475.05(17) <sup>b</sup>
$\bar{a}_l$ (nm)	1.45 <sup>d</sup>		1.67 <sup>d</sup>	0.967 <sup>d</sup>
$Q$ (b)	+0.307(4) <sup>e</sup>	-0.41(4) <sup>e</sup>	-0.49(5) <sup>e</sup>	-0.58(9) <sup>e</sup>

<sup>a</sup> Feher (Ref. 15)

<sup>b</sup> Mortemousque *et al.* (Ref. 39)

<sup>c</sup> Wolfowicz *et al.* (Ref. 10)

<sup>d</sup> Pica *et al.* (Ref. 27)

<sup>e</sup> Stone (Ref. 49)

tallographic [001] direction.

The Bi donor can be modeled by the spin Hamiltonian

$$\hat{\mathcal{H}} = g_e \mu_B B_z \hat{S}_z - g_n \mu_N B_z \hat{I}_z + h A \hat{S} \cdot \hat{I} + \hat{I} Q \hat{I}, \quad (1)$$

where  $g_e$  and  $g_n$  are the donor electron and nuclear  $g$ -factors, respectively,  $A$  is the strength of the isotropic hyperfine interaction (see Table I), and  $B_z$  is the magnetic field in a  $z$  direction. The eigenstates  $|i\rangle$  of Eq. (1) are labeled in order of increasing energy [50]. The term  $\hat{I} Q \hat{I}$  represents the donor nuclear spin QI with an EFG. For an electrostatic field  $E_z$  experienced by the nucleus in presence of the electronic charge configuration of its atom, the EFG in  $z$  direction is  $\partial E_z / \partial z = V_{zz}^{\text{eff}}$ , and the QI is written [28]

$$\hat{I} Q \hat{I} = \nu_Q \left( 3 \hat{I}_z^2 - I(I+1) \right) / (4I(2I-1)), \quad (2)$$

where the coefficient  $\nu_Q = h e Q V_{zz}^{\text{eff}}$ ,  $e$  is the elementary electrical charge and  $Q$  is the quadrupole moment of the nucleus.

When working at high magnetic fields, the eigenstates of Eq. (1) are given by the products of the electron and nuclear spin states. In this case, their magnetic resonances are addressed separately, either in ESR ( $\Delta m_I = 0$ ,  $\Delta m_S = \pm 1$ , where  $m_I$  and  $m_S$  are the eigenvalues of  $\hat{I}_z$  and  $\hat{S}_z$ ) or NMR ( $\Delta m_S = 0$ ,  $\Delta m_I = \pm 1$ ). In SDR spectroscopy, which is sensitive to the electron spin configuration, only terms involving the electron spin operator  $\hat{S}$  can be detected, namely the electron Zeeman interaction and the hyperfine interaction. For  $hA \gtrsim g_e \mu_B B_z$ , however, the eigenstates are linear combinations of several nuclear and electron states, so-called mixed states [51, 52]. Resonant transitions which change both spin states become possible, allowing for transitions which are sensitive to the nuclear spin properties but also change the electron spin state to become detectable by SDR [38, 53]. The sensitivity of low-field line positions to the different constants describing the spin system is given by the corresponding

derivatives, which were calculated numerically and are given for  $^{209}\text{Bi}$  in Fig. 1(b). The spin-dependent conductivity signal is based on weakly coupled spin pairs, which are most efficiently formed for ‘pure’ electron spin states [38, 51]. The transitions most easily detected [see Fig. 1(a, b)] are therefore those involving the two product states:  $|\uparrow\rangle|\uparrow\rangle = |m_S = +S\rangle|m_I = +I\rangle$  ( $|19\rangle \leftrightarrow |20\rangle$ , in blue) and  $|\downarrow\rangle|\downarrow\rangle = |m_S = -S\rangle|m_I = -I\rangle$  ( $|10\rangle \leftrightarrow |11\rangle$  in green). Other NMR-like transitions have a weak SDR intensity [Fig. 1(c)].

The EPR and NMR transition frequencies of Bi donors are plotted in Fig. 1(a) as a function of magnetic field. Figure 1(c) shows an SDR spectrum of  $^{209}\text{Bi}$  donors in silicon recorded under a 200-MHz excitation. Four of the observed peaks are identified as the resonance transitions induced by the X-band microwave (9.086 GHz) employed for the detection of the ac-conductivity of the sample. They can be used to extract the electron  $g$ -factor and the hyperfine interaction  $A$  since they are, in good approximation, not influenced by the nuclear Zeeman interaction or the QI [see Fig. 1(b)]. As discussed in Ref. 51, the observed values are slightly different from those observed in conventional ESR due to influence of the recombination partner. Other possible explanations might be the presence of strain [16] or Stark shift [22, 27] induced by charged defects. In addition, several peaks are observed due to the rf excitation, in particular two prominent lines at  $\sim 550$  G and  $\sim 960$  G which are attributed to the NMR-like transitions involving pure electron spin states  $|10\rangle \leftrightarrow |11\rangle$  and  $|19\rangle \leftrightarrow |20\rangle$ , respectively. However, when comparing these to the line positions as calculated for Eq. (1) using the values for  $A$  and  $g_e$  extracted from the X-band line positions and with zero QI indicated by the NMR bar ticks in Fig. 1(c), the NMR lines appear to be shifted significantly.

To gain further insight into the origin of the observed shift, the resonance lines are recorded at different excitation frequencies as shown in Fig. 2(c) where the horizontal axes are aligned to the expected resonance field  $B_0^{\text{th}}$  for the spin system without QI. For all the measured NMR spectra of Si: $^{209}\text{Bi}$ , the detuning of the resonant magnetic field for three transitions as a function of the magnetic field is shown in Fig. 2(a). Since the observed shifts are orders of magnitude larger than could be expected for a change in nuclear  $g$ -factor, we will now discuss the nuclear QI as a possible explanation. To separate the effect of the QI from other possible influences, the data points are plotted as a function of  $\partial B/\partial\nu_Q$  of the corresponding transitions [Fig. 2(b)]. The line positions extracted from the  $|19\rangle \leftrightarrow |20\rangle$ ,  $|10\rangle \leftrightarrow |11\rangle$  and  $|1\rangle \leftrightarrow |2\rangle$  transitions are well described by a linear dependence, which confirms the QI of the nucleus as origin of the observed shift. The linear fit slopes of the experimental data of Fig. 2(b) indicates a QI  $\nu_{\text{QBi}}^{\text{exp}} = -18.2(2)$  MHz in Si: $^{209}\text{Bi}$ . The corresponding effective EFG is  $V_{zz}^{\text{eff,Bi}} = 1.3 \times 10^{21}$  V/m $^2$ .

However, an additional constant offset is necessary to reproduce the experimentally observed line shifts. A

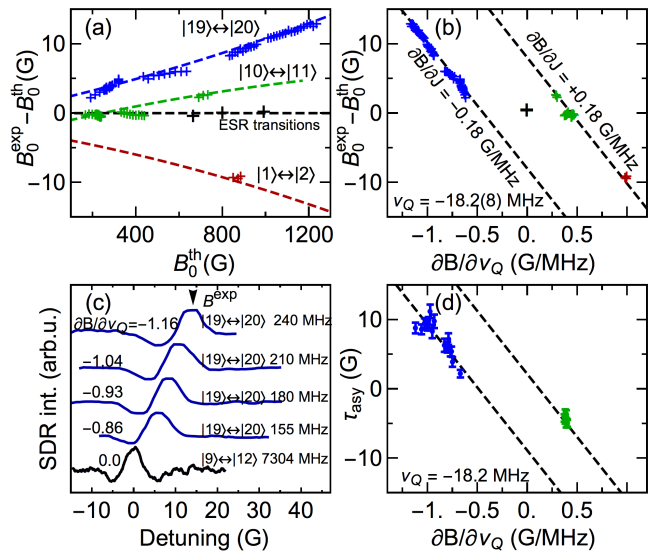


FIG. 2. (Color online.) Detuning  $B_0^{\text{exp}} - B_0^{\text{th}}$  of the transitions  $|19\rangle \leftrightarrow |20\rangle$  (blue crosses),  $|10\rangle \leftrightarrow |11\rangle$  (green crosses), and  $|1\rangle \leftrightarrow |2\rangle$  (red crosses) of Si: $^{209}\text{Bi}$  plotted as a function of the magnetic field (a) and the sensitivity  $\partial B/\partial\nu_Q$  (b) giving an exchange interaction  $J = 45$  MHz. The black points correspond to the  $|1\rangle \leftrightarrow |20\rangle$ ,  $|2\rangle \leftrightarrow |19\rangle$  and  $|3\rangle \leftrightarrow |18\rangle$  X-band ESR transitions. (c) Experimentally observed SDR spectra of the Bi spin transitions  $|19\rangle \leftrightarrow |20\rangle$  (blue) recorded at various frequencies (corresponding to different sensitivities  $\partial B/\partial\nu_Q$ ). The spectrum (black) of the  $|9\rangle \leftrightarrow |12\rangle$  transition, recorded at the hyperfine clock transition [39] (insensitive to changes in hyperfine and only weakly to QI) at 7304 MHz, is plotted for comparison. The  $x$ -axis is the detuning of the considered spin transition  $B_0^{\text{exp}} - B_0^{\text{th}}$  where  $B_0^{\text{exp}}$  is the measured resonant field and  $B_0^{\text{th}}$  is the resonant field calculated assuming that  $\nu_Q = 0$  in Eq. (1). (d) Asymmetry parameter  $\tau_{\text{asy}}(\partial B/\partial\nu_Q)$  (see text) plotted for Si:Bi spectra (with high enough signal and non overlapping peaks). The dashed lines are guides for this eye with a slope of  $-18.2$  MHz.

possible explanation could be the exchange interaction ( $J \vec{S}_R \cdot \vec{S}$ ) between the readout partner (electron spin state  $m_R$ ) and the donor electron spins which was not considered in Eq. (1) and leads to a constant shift of the resonance for the transitions and frequency region considered here. This is supported by the different signs of the offsets observed for the three transitions, in agreement with the steady state polarization of the spin pairs due to the spin-dependent recombination. With the expected sensitivity  $\partial B/\partial J = -m_R \frac{h}{g_e \mu_B} \approx -0.18$  G/MHz for  $|19\rangle \leftrightarrow |20\rangle$  ( $+0.18$  for  $|10\rangle \leftrightarrow |11\rangle$  and  $|1\rangle \leftrightarrow |2\rangle$ ), the observed  $\mp 8.0(4)$  G offsets in Fig. 2(b) could be explained by a coupling constant  $J(\text{Bi}) = 45(2)$  MHz, significantly stronger than usually observed in SDR experiments [54]. Another possible cause to this offset might be the asymmetric and broad distribution of the QI (assumed to be exponential in this study). Figure 2(d) shows that the

parameter  $\tau_{\text{asy}}$  of the fitting function

$$\frac{d^2 \{ \exp(-B/\tau_{\text{asy}}) \otimes \exp(-(B - B^{\text{exp}})^2/2\sigma^2) \}}{dB^2} \quad (3)$$

scales with  $\partial B/\partial\nu_Q$ . The offsets of these curves indicate that the asymmetry of the resonance peaks is not only caused by QI, but possibly by exchange interaction as well.

In order to investigate further the origin of the EFG responsible for the QI, we reproduced the same measurement protocol with antimony donors in silicon, which have a different Bohr radius than Bi donors, allowing us to characterize the role of the donor electron distribution in the generation of the EFG. Figure 3(a) [respectively (b)] shows the experimentally measured shift of NMR-like transitions of  $^{121}\text{Sb}$  [ $^{123}\text{Sb}$ ] donors against  $\partial B/\partial\nu_Q$ . A linear fit of the points indicates a QI  $\nu_Q^{\text{exp}}(^{121}\text{Sb}) = -2.9(1)$  MHz and  $\nu_Q^{\text{exp}}(^{123}\text{Sb}) = -2.95(2)$  MHz, and an exchange interaction of  $J(^{121}\text{Sb}) = 13(2)$  MHz and  $J(^{123}\text{Sb}) = 20(3)$  MHz.

Similarly to the Si:Bi asymmetry fitting parameter,  $\tau_{\text{asy}}(^{121}\text{Sb})$  has an offset at  $\partial B/\partial\nu_Q = 0$  implying that the line asymmetry is not only due to QI [see Fig. 3(c)]. The quadrupole moment ratio  $Q_{^{121}\text{Sb}}/Q_{^{123}\text{Sb}}$  is 0.84. An equivalent ratio would be expected for  $\nu_Q^{\text{exp}}(^{121}\text{Sb})/\nu_Q^{\text{exp}}(^{123}\text{Sb})$ , but the experimentally observed ratio is  $\approx 1$ . This suggests that the observed shift is influenced by other parameters as well. Further studies, for example with electron nuclear double resonance experiments in the high-field limit, could help to identify the effects on nuclear and electron spin resonances more clearly. Though the definite quantitative explanation of the observed line positions will have to be left for future studies, our experiments indicate QI in the order of several MHz, corresponding to EFG on the order of  $10^{20}$  V/m<sup>2</sup>.

No external control of the EF or of the EFG was per-

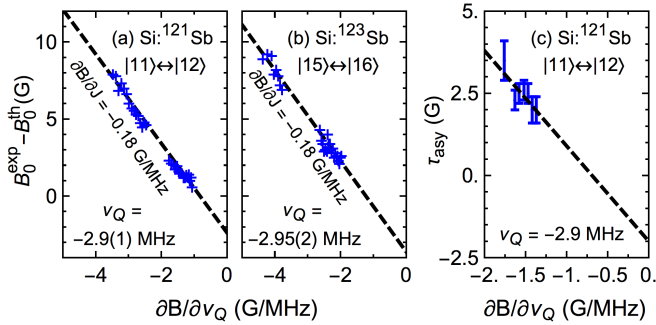


FIG. 3. (Color online.) Detuning, as defined in Fig. 2, of the resonant field observed for various nuclear spin-like transitions of Si: $^{121}\text{Sb}$  (a) and Si: $^{123}\text{Sb}$  (b) plotted as a function of the sensitivity  $\partial B/\partial\nu_Q$ . The linear fits indicate a QI of  $\nu_Q = -2.9(1)$  MHz for Si: $^{121}\text{Sb}$  and  $\nu_Q = -2.95(2)$  MHz for Si: $^{123}\text{Sb}$ . (c) Asymmetry parameter  $\tau_{\text{asy}}(\partial B/\partial\nu_Q)$  (see text) plotted for the Si: $^{121}\text{Sb}$  spectra. The dashed line is a guide for the eyes with a slope of  $-2.9$  MHz.

formed during the experiments and the EFG induced by local strain [31] is assumed to be negligible as no evidence of strain could be found in the Si:Bi sample [39] nor in the Si:Sb samples at X-band. Therefore, we base our model on the hypothesis that the EFG at the nucleus is induced by a redistribution of the donor electron density. In order to confirm this hypothesis, we proceeded in two steps. First, the orbital of the donor-readout center electron pair can be modeled in order to evaluate the mixing of the different valleys of the donor 1s ground state. This was performed using a variational calculation using the six donor valley configurations of the 1s state plus a localised readout center as the wave functions basis [39]. The energy levels of the donor ground states are known from optical studies [55], whereas the localised readout center energy level is assumed to be  $E_R = -0.25$  eV [56]. The envelop functions were calculated using a corrected effective mass theory donor wave function. The parameter  $\eta = 159.4$  described in Ref. 57 was used to adjust the envelop functions close to the donor nucleus [58]. Due to the presence of the readout center, the different valley populations of the donor ground state adjust to become  $\psi = \alpha_{A1}\phi_{A1} + \sum \alpha_i\phi_i$ , where  $\phi_i$  are the two-fold E and three-fold T<sub>2</sub> valley configurations and  $\alpha_{A1}^2 + \sum \alpha_i^2 = 1$ . The coefficients  $\alpha_i$  depend strongly on the distance between the two recombination partners, as well as their relative orientation with respect to the crystal axes.

The second step was the computation of the EFG for each donor valley configuration. One can express the EFG  $V_{x_ix_i}$  generated by an orbital  $\psi$  as [28]

$$V_{x_ix_i} = \langle \psi | \hat{\mathcal{H}}_{x_ix_i}^{\text{orb}} | \psi \rangle = \frac{e}{4\pi\epsilon_0\epsilon_{\text{Si}}} \int \psi^* \frac{3x_i^2 - r^2}{r^5} \psi \, d\tau, \quad (4)$$

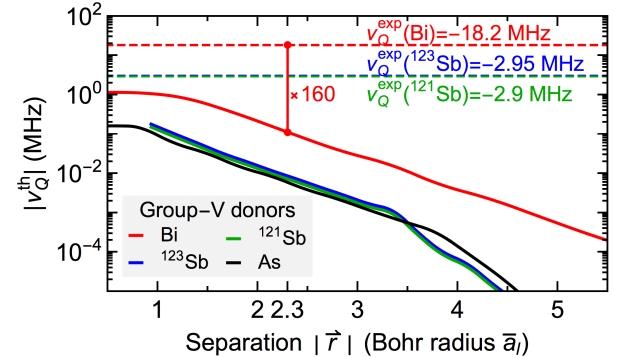


FIG. 4. (Color online.) Simulation of the QI maximum (see text) plotted for group-V donors ( $I > 1$ ) in silicon as functions of the D-R pair separation (the readout center can occupy any 3-dimensional lattice site). The pair separation  $r$  is calculated in units of the donors Bohr radius  $\bar{a}_l$ , as in Ref. 27. The As quadrupole moment  $Q$  is positive, leading to a positive  $\nu_Q^{\text{th}}(\text{As})$ , whereas  $^{121}\text{Sb}$ ,  $^{123}\text{Sb}$  and  $^{209}\text{Bi}$  quadrupole moments are negative, leading to negative  $\nu_Q^{\text{th}}(^{121}\text{Sb})$ ,  $\nu_Q^{\text{th}}(^{123}\text{Sb})$  and  $\nu_Q^{\text{th}}(\text{Bi})$ . For clarity, only the absolute values are plotted.

TABLE II. Simulated values, using Eq. (4), of the EFG for different valley configurations for each group-V donors with  $I > 1$ . Only values of EFG larger than  $10^{15} \text{ V/m}^2$  are shown (numerical integration precision threshold). The EFG numerical values are given in units of  $10^{19} \text{ V/m}^2$ . We use the valley notation  $A_1$ :  $(X + \bar{X} + Y + \bar{Y} + Z + \bar{Z})/\sqrt{6}$ ,  $E_{x,y}$ :  $(X + \bar{X} - Y - \bar{Y})/2$ , and  $E_{2z}$ :  $(2Z + 2\bar{Z} - X - \bar{X} - Y - \bar{Y})/\sqrt{12}$ .  $^{121}\text{Sb}$  and  $^{123}\text{Sb}$  donors have the same donor electron orbital, noted Si:Sb.

	Si:As	Si:Sb	Si:Bi
$\langle A_1   \hat{\mathcal{H}}_{xx}^{\text{orb}}   E_{x,y} \rangle$	3.0	2.7	11.6
$\langle A_1   \hat{\mathcal{H}}_{zz}^{\text{orb}}   E_{x,y} \rangle$	0	0	0
$\langle A_1   \hat{\mathcal{H}}_{xx}^{\text{orb}}   E_{2z} \rangle$	-1.7	-1.6	-6.7
$\langle A_1   \hat{\mathcal{H}}_{zz}^{\text{orb}}   E_{2z} \rangle$	3.4	3.2	13.4

where  $x_i = x, y, z$ . Therefore, the first order term of the EFG is of the form  $\alpha_i \langle A_1 | \hat{\mathcal{H}}^{\text{orb}} | \phi_i \rangle$ . The first order EFG perturbative term was found to be significant only for the E-doublet valley configuration (the second and higher order correction terms are negligible). The different matrix elements calculated in this work are shown in Table II.

Figure 4 shows the simulation results of the maxima of  $\nu_Q^{\text{th}}$  (for the quantization axis along the D–R separation direction) among all possible lattice sites within a shell of radius  $r$ . The QI for the group-V donors in silicon with a nuclear spin  $I > 1$  are plotted as a function of the separation  $|\vec{r}|$  (normalised by the Bohr radius  $\bar{a}_l$  of each donor species) between the donor and readout center. For Bi donors, the average separation  $r$  has been calculated to be  $2.3 \bar{a}_l$  [39], leading to an EFG underestimated by a factor  $\nu_Q^{\text{exp}}(\text{Bi})/\nu_Q^{\text{th}}(\text{Bi}) = 160$ . This factor might be explained by the presence of several defects in the vicinity of a donor, leading to an underestimation of the orbital mixing estimated in this study. Another possible cause might be the antishielding phenomenon. Upon application of an EFG, the energy levels of all shells of an ion or an atom are modified, giving rise to an induced EFG by the subshell electrons. Feiock and Johnson [59] have shown that a first order correction to the subshell energy levels leads to a linear correction of the EFG so that  $V_{zz}^{\text{tot}} = (1 - \gamma)V_{zz}^{\text{eff}}$ , where  $V_{zz}^{\text{tot}}$  is the EFG at the donor nucleus. The parameter  $\gamma$  is called the

antishielding or Sternheimer coefficient. The antishielding parameters of donors in silicon have been measured only for limited species and ionization numbers. A donor forms four covalent bonds with the nearby Si atoms, and its core electron shells are therefore close to  $\text{D}^{5+}$  plus the contribution of the four covalent electrons. For Bi donors [59],  $\gamma(\text{Bi}^{5+}) = -47.24$  and the effect of the four covalent bonds would be to reduce this value down to  $-159$ . As Bi donor and Sb donors have different number of core electrons, the antishielding parameters may be very different. The determination of the antishielding parameters is beyond the scope of this work and is left for further studies.

The QI with a uniaxial EFG shows a strong dependence on the angle between gradient axis and magnetic field [60], which is in first order  $(3 \cos^2 \theta - 1)/2$ . For our calculations, the tetrahedral symmetry of the donor is broken by the presence of a defect center. For a random distribution of defect sites, one expects a continuous distribution of  $h\mathcal{Q}V_{zz}$  from  $-\nu_Q/2$  to  $\nu_Q$ . The second harmonic lock-in detection of the change in the sample conductivity used in this study allows us to detect only the edge of the broadened resonance peaks. Therefore a continuous distribution in  $V_{zz}$  would lead to a peak splitting. In our experiments no clear evidence of such splitting could be observed. Angular dependence experiments of the frequency shift might help to clarify this issue.

In summary, we have observed a shift of NMR-like transitions for Bi and Sb donors in Si and their probable link to QI. We have analyzed, using a molecular orbital model, the mixing of the donors ground states as a possible origin of the EFG. Finally, we have discussed an alternative to the presence of a readout center for mixing the donor electron orbital to generate EFGs and, as a consequence, quadrupole interactions.

*Acknowledgments* The authors thank J. Pla for discussions. This work has been supported in part by the JSPS Core-to-Core program, in part by the Grants-in-Aid for Scientific Research by MEXT, and in part by NanoQuine. GP was funded by the joint EPSRC (EP/I035536) / NSF (DMR-1107606) Materials World Network grant. We also acknowledge access to NCRIS facilities (ANFF and the Heavy Ion Accelerator Capability) at the Australian National University.

---

[1] B. E. Kane, Nature **393**, 133 (1998).  
[2] T. D. Ladd, D. Maryenko, Y. Yamamoto, E. Abe, and K. M. Itoh, Phys. Rev. B **71**, 014401 (2005).  
[3] A. M. Tyryshkin, J. J. L. Morton, S. C. Benjamin, A. Ardashyan, G. A. D. Briggs, J. W. Ager, and S. A. Lyon, J. Phys.: Condens. Matter **18**, S783 (2006).  
[4] K. Takyu, K. M. Itoh, K. Oka, N. Saito, and V. I. Ozhogin, Jpn. J. Appl. Phys. **38**, L1493 (1999).  
[5] B. Andreas, Y. Azuna, G. Bartl, P. Becker, H. Bettin, M. Borys, I. Busch, M. Gray, P. Fuchs, K. Fujii, H. Fujimoto, E. Kessler, M. Krumrey, U. Kuettgens, N. Kuramoto, G. Mana, P. Manson, E. Massa, S. Mizushima, A. Nicolaus, A. Picard, A. Pramann, O. Rienitz, D. Schiel, S. Valkiers, and A. Waseda, Phys. Rev. Lett. **106**, 030801 (2011).  
[6] K. M. Itoh and H. Watanabe, MRS Comm. **4**, 143 (2014).  
[7] E. Abe, A. M. Tyryshkin, S. Tojo, J. J. L. Morton, W. M. Witzel, A. Fujimoto, J. W. Ager, E. E. Haller, J. Isoya, S. A. Lyon, M. L. W. Thewalt, and K. M. Itoh, Phys. Rev. B **82**, 121201(R) (2010).

[8] A. M. Tyryshkin, S. Tojo, J. J. L. Morton, H. Riemann, N. V. Abrosimov, P. Becker, H. J. Pohl, T. Schenkel, M. L. W. Thewalt, K. M. Itoh, and S. A. Lyon, *Nat. Mater.* **11**, 143 (2012).

[9] M. Steger, K. Saeedi, M. L. W. Thewalt, J. J. L. Morton, H. Riemann, N. V. Abrosimov, P. Becker, and H. J. Pohl, *Science* **336**, 1280 (2012).

[10] G. Wolfowicz, A. M. Tyryshkin, R. E. George, H. Riemann, N. V. Abrosimov, P. Becker, H. J. Pohl, M. L. W. Thewalt, S. A. Lyon, and J. J. L. Morton, *Nat. Nanotechnol.* **8**, 561 (2013).

[11] K. Saeedi, S. Simmons, J. Z. Salvail, P. Dluhy, H. Riemann, N. V. Abrosimov, P. Becker, H. J. Pohl, J. J. L. Morton, and M. L. W. Thewalt, *Science* **342**, 830 (2013).

[12] A. Morello, J. J. Pla, F. A. Zwanenburg, K. W. Chan, K. Y. Tan, H. Huebl, M. Mottonen, C. D. Nugroho, C. Yang, J. A. van Donkelaar, A. D. C. Alves, D. N. Jamieson, C. C. Escott, L. C. L. Hollenberg, R. G. Clark, and A. S. Dzurak, *Nature* **467**, 687 (2010).

[13] J. J. Pla, K. Y. Tan, J. P. Dehollain, W. H. Lim, J. J. L. Morton, D. N. Jamieson, A. S. Dzurak, and A. Morello, *Nature* **489**, 541 (2013).

[14] J. T. Muhonen, J. P. Dehollain, A. Laucht, F. E. Hudson, R. Kaira, T. Sekiguchi, K. M. Itoh, D. N. Jamieson, J. C. McCallum, A. S. Dzurak, and A. Morello, *Nat. Nanotechnol.* **9**, 986 (2014).

[15] G. Feher, *Phys. Rev.* **114**, 1219 (1959).

[16] D. K. Wilson and G. Feher, *Phys. Rev.* **124**, 1068 (1961).

[17] E. B. Hale and R. L. Mieher, *Phys. Rev.* **184**, 739 (1969).

[18] R. A. Faulkner, *Phys. Rev.* **184**, 713 (1969).

[19] J. L. Ivey and R. L. Mieher, *Phys. Rev. B* **11**, 822 (1975).

[20] F. R. Bradbury, A. M. Tyryshkin, G. Sabouret, J. Bokor, T. Schenkel, and S. A. Lyon, *Phys. Rev. Lett.* **97**, 176404 (2006).

[21] C. C. Lo, S. Simmons, R. Lo Nardo, C. D. Weis, A. M. Tyryshkin, J. Meijer, D. Rogalla, S. A. Lyon, J. Bokor, T. Schenkel, and J. J. L. Morton, *Appl. Phys. Lett.* **104**, 193502 (2014).

[22] G. Wolfowicz, M. Urdampilleta, M. L. W. Thewalt, H. Riemann, N. V. Abrosimov, P. Becker, H. J. Pohl, and J. J. L. Morton, *Phys. Rev. Lett.* **113**, 157601 (2014).

[23] G. D. J. Smit, S. Rogge, J. Caro, and T. M. Klapwijk, *Phys. Rev. B* **70**, 035206 (2004).

[24] M. Friesen, *Phys. Rev. Lett.* **94**, 186403 (2005).

[25] R. Rahman, C. J. Wellard, F. R. Bradbury, M. Prada, J. H. Cole, G. Klimeck, and L. C. L. Hollenberg, *Phys. Rev. Lett.* **99**, 036403 (2007).

[26] R. Rahman, S. H. Park, T. B. Boykin, G. Klimeck, S. Rogge, and L. C. L. Hollenberg, *Phys. Rev. B* **80**, 155301 (2009).

[27] G. Pica, G. Wolfowicz, M. Urdampilleta, M. L. W. Thewalt, H. Riemann, N. V. Abrosimov, P. Becker, H. J. Pohl, J. J. L. Morton, R. N. Bhatt, S. A. Lyon, and B. W. Lovett, *Phys. Rev. B* **90**, 195204 (2014).

[28] E. N. Kaufmann and R. J. Vianden, *Rev. Mod. Phys.* **51**, 161 (1979).

[29] D. Y. Jeon, J. F. Donegan, and G. D. Watkins, *Phys. Rev. B* **39**, 3207 (1989).

[30] H. Kotegawa, K. Fukumoto, T. Toyama, H. Tou, H. Harima, A. Harada, Y. Kitaoka, Y. Haga, E. Yamamoto, Y. Onuki, K. M. Itoh, and E. E. Haller, *J. Phys. Soc. Jap.* **84**, 054710 (2015).

[31] D. P. Franke, F. M. Hrubesch, M. Künzl, K. M. Itoh, M. Stutzmann, F. Hoehne, L. Dreher, and M. S. Brandt, arXiv:1503.00133v1 (2015).

[32] J. Ishihara, M. Ono, G. Sato, S. Matsuzaka, Y. Ohno, and H. Ohno, *Jap. J. Appl. Phys.* **53**, 093001 (2014).

[33] A. Burchard, M. Deicher, V. N. Fedoseyev, D. Forkel-Wirth, R. Magerle, V. I. Mishin, D. Steiner, A. Stotzler, R. Weissenborn, T. Wickert, and the ISOLDE-Collaboration, *Hyperfine Interactions* **120**, 389 (1999).

[34] E. L. Elkin and G. D. Watkins, *Phys. Rev.* **174**, 881 (1968).

[35] G. D. Watkins, *Mat. Res. Soc. Symp. Proc.* **469**, 139 (1997).

[36] A. Nylandsted Larsen, A. Mesli, K. Bonde Nielsen, H. Kortegaard Nielsen, L. Dobaczewski, J. Adey, R. Jones, D. W. Palmer, P. R. Briddon, and S. Oberg, *Phys. Rev. Lett.* **97**, 106402 (2006).

[37] D. J. Lepine, *Phys. Rev. B* **6**, 436 (1972).

[38] P. A. Mortemousque, T. Sekiguchi, C. Culan, M. P. Vlasenko, R. G. Elliman, L. S. Vlasenko, and K. M. Itoh, *Appl. Phys. Lett.* **101**, 082409 (2012).

[39] P. A. Mortemousque, S. Berger, T. Sekiguchi, C. Culan, R. G. Elliman, and K. M. Itoh, *Phys. Rev. B* **89**, 155202 (2014).

[40] F. A. Trumbore, *Bell Syst. Tech.* **39**, 205 (1959).

[41] P. Studer, S. R. Schofield, C. F. Hirjibehedin, and N. J. Curson, *Appl. Phys. Lett.* **102**, 012107 (2013).

[42] O. J. Marsh, R. Baron, G. A. Shifrin, and J. W. Mayer, *Appl. Phys. Lett.* **13**, 199 (1968).

[43] R. Baron, G. A. Shifrin, O. J. Marsh, and J. W. Mayer, *J. Appl. Phys.* **40**, 3702 (1969).

[44] J. P. de Souza and P. F. P. Fichtner, *J. Appl. Phys.* **74**, 119 (1993).

[45] C. D. Weis, C. C. Lo, V. Lang, A. M. Tyryshkin, R. E. George, K. M. Yu, J. Bokor, S. A. Lyon, J. J. L. Morton, and T. Schenkel, *Appl. Phys. Lett.* **100**, 172104 (2012).

[46] Y. Ochiai and E. Matsuura, *Phys. Stat. Sol. A* **27**, K89 (1975).

[47] E. Abramof, A. Ferreira da Silva, B. E. Sernelius, J. P. de Souza, and H. Boudinov, *Phys. Rev. B* **55**, 9584 (1997).

[48] F. Hoehne, L. Dreher, M. Suckert, D. P. Franke, M. Stutzmann, and M. S. Brandt, *Phys. Rev. B* **88**, 155301 (2013).

[49] N. J. Stone, *Atom. Data and Nucl. Data Tables* **90**, 75 (2005).

[50] M. H. Mohammady, G. W. Morley, and T. S. Monteiro, *Phys. Rev. Lett.* **105**, 067602 (2010).

[51] H. Morishita, L. S. Vlasenko, H. Tanaka, K. Semba, K. Sawano, Y. Shiraki, M. Eto, and K. M. Itoh, *Phys. Rev.* **80**, 205206 (2009).

[52] L. Dreher, F. Hoehne, H. Morishita, H. Huebl, M. Stutzmann, K. M. Itoh, and M. S. Brandt, *Phys. Rev. B* **91**, 075314 (2015).

[53] D. Franke, M. Otsuka, T. Matsuoka, L. S. Vlasenko, M. P. Vlasenko, M. S. Brandt, and K. M. Itoh, *Appl. Phys. Lett.* **105**, 112111 (2014).

[54] M. Suckert, F. Hoehne, L. Dreher, M. Kuenzl, M. Huebl, H. Stutzmann, and M. S. Brandt, *Molecular Physics* **111**, 2690 (2013).

[55] A. K. Ramdas and S. Rodriguez, *Rep. Prog. Phys.* **44**, 1297 (1981).

[56] E. H. Poindexter, G. J. Gerardi, M. E. Rueckel, P. J. Caplan, N. M. Johnson, and D. K. Biegelsen, *J. Appl. Phys.* **56**, 2844 (1984).

- [57] L. V. C. Assali, H. M. Petrili, R. B. Capaz, B. Koiler, X. Hu, and S. Das Sarma, Phys. Rev. B **83**, 165301 (2011).
- [58] W. Kohn and J. M. Luttinger, Phys. Rev. **97**, 883 (1955).
- [59] F. D. Feiock and W. R. Johnson, Phys. Rev. **187**, 39 (1969).
- [60] M. H. Levitt, *Spin dynamics: Basics of Nuclear Magnetic Resonance* (John Wiley & Sons Ltd., Chichester, 2008).